

Modelling, Analysis and Control of Blowing-Venting Operations in Manned Submarines

Roberto Font¹, Javier García-Peláez², José A. Murillo³, Francisco Periago⁴

^{1,3,4}Department of Applied Mathematics and Statistics, Universidad Politécnica de Cartagena, 30202 Cartagena, Spain

²Direction of Engineering, DICA, Navantia S.A., 30205 Cartagena, Spain

¹roberto.font@gmail.com; ²jpgpelaez@navantia.es; ³alberto.murillo@upct.es ⁴f.periago@upct.es

Abstract- Motivated by the study of the potential use of blowing and venting operations of ballast tanks in manned submarines as a complementary or alternative control system for manoeuvring, we first propose a mathematical model for these operations. Then we consider the coupling of blowing and venting with the Feldman, variable mass, coefficient based hydrodynamic model for the equations of motion. The final complete model is composed of a system of twenty-four nonlinear ordinary differential equations. In a second part, we carry out a rigorous mathematical analysis of the model: existence of a solution is proved. As one of the possible applications of this model in naval engineering problems, we consider the problem of roll control in an emergency rising manoeuvre by using only blowing and venting. To this end, we formulate a suitable constrained, nonlinear, optimal control problem where controls are linked to the variable aperture of blowing and venting valves of each of the tanks. Existence of a solution for this problem is also proved. Finally, we address the numerical resolution of the control problem by using a descent algorithm. Numerical experiments seem to indicate that, indeed, an appropriate use of blowing and venting operations may help in the control of this emergency manoeuvre.

Keywords- Ballast Tanks; Manned Submarines; Blowing-Venting Operations; Optimal control; Numerical Simulations.

I. INTRODUCTION

Manned submarines are equipped with several ballast tanks distributed along its hull. When filled with water, they contribute with the submarine mass allowing it to submerge. During an unexpected event or emergency, like on board fire or flood, they act as a safety mechanism to drive the vehicle to the surface: air is blown into the ballast tanks from very high pressure bottles expelling the water out of the tanks. The submarine loses weight, its buoyancy is higher, and it can emerge quicker. In the last years, several works have addressed these emergency rising manoeuvres (see [1, 2, 17, 18] and the references given there). To fill the tanks with water again, air is vented out of the ballast tanks. A valve located at the top of each of the tanks is opened, air escapes outside, and water flows back into the tanks.

Emergency blowing is considered a potentially dangerous manoeuvre and is seldom performed in full scale tests. The very high costs associated with scale model tests, on the other hand, make them prohibitive for many navies and, in any case, suitable only for the later stages of development. In this context, numerical simulation becomes a much more affordable alternative and an extremely useful tool, particularly during the preliminary stages of design or to test new concepts.

Our first aim in this paper is to obtain a mathematical model for the blowing and venting processes and their influence on vehicle motion. The ability to simulate manoeuvres involving blowing and venting can serve naval architects to a) fit several parameters of ballasting and deballasting systems (such as size of ballast tanks and/or blowing and venting valves) during the preliminary state of design of a prototype and b) improve the understanding of the emergency manoeuvres and its associated difficulties.

The issue of modelling the blowing of ballast tanks has been addressed, for instance, in [2] and [18]. Up to the best knowledge of the authors, venting has not been addressed so far, and most importantly, the coupling of both processes as a control system has not been considered before. In Section II we propose a model for a coupled system of blowing-venting operations. For the particular case where only blowing is considered, the model presented in this work was numerically compared in [7] with the one proposed by Watt [18] giving similar results, but also showing the ability to capture some phenomena that were overlooked by that last model. Then, these two processes are coupled with the usual Feldman's coefficient based hydrodynamic model for the equations of motion (see [6] and more precisely [11]) which, although some more accurate models such as the one considered in [13] are being considered in the literature, are the standard in manned submarines. We notice that, since the mass of the submarine changes with blowing-venting operations, some of the parameters (e.g., moments and products of inertia, weight, mass, etc...) that remain constant in Feldman's model are, in our case, time dependent. However, as it is usual in manned submarines (see for instance [17, 18]) and also in surface ships [10], our model is a quasi-steady variable mass model in the sense that the term dm/dt which appears in Newton's second law is neglected. A justification of this fact is included at the end of Subsection II.B.

Our second objective is to analyze the effectiveness of blowing-venting operations as a complementary control mechanism. Indeed, buoyancy control could improve performance during rising manoeuvres and also be an invaluable tool when the control surfaces are not effective due to the low (or vanishing) vehicle velocity. This is the case of underwater hovering, the action of statically keep a desired depth. For manned submarines, accurate hovering is essential, for example, for safe swimmers delivery, cover supply replacement or the deployment and recovery of AUVs. As a first step in this direction, we test the ability of

blowing-venting control to improve roll stability during a typical emergency manoeuvre. To this end, in Section III we model such a manoeuvre as a constrained, nonlinear, optimal control problem which has the aperture of blowing-venting valves of each of the tanks as the control variables. The underlying state law is composed of a nonlinear system of $3N + 12$ ordinary differential equations (ODE's), where N is the number of ballast tanks.

The mathematical analysis of the model is presented in Section IV. Finally, for the numerical resolution of the optimal control problem we use an open loop approach which is enough to comply with the goals a) and b) described above. Precisely, we implement a gradient descent method as in [11]. The performance of the algorithm is illustrated in Section V through the numerical simulation of an emergency manoeuvre. Results seem to indicate that blowing-venting operations may help in a significant way to the control of this type of manoeuvres.

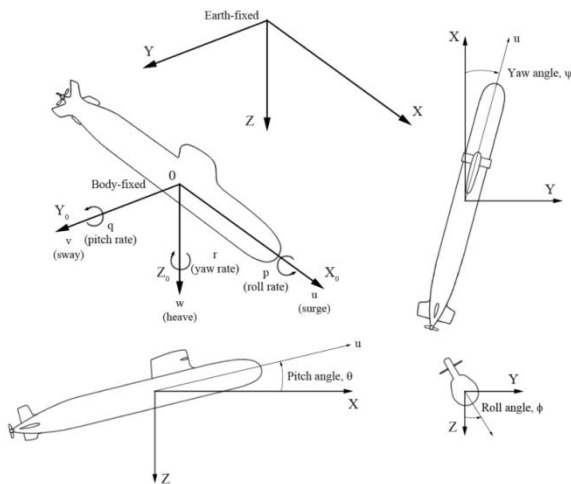


Fig. 1 Variables and coordinate systems.

II. MATHEMATICAL MODELLING

The three-dimensional equations of motion for an underwater vehicle are usually described by using two coordinate frames: the moving coordinate frame which is fixed to the vehicle and is called the body-fixed system, and the earth-fixed reference frame which is called the world system. The position and orientation of the vehicle are described in the world system while the linear and angular velocities are expressed in the body-fixed coordinate system. These quantities are defined according to SNAME notation [9] as

$$\boldsymbol{\eta}(t) = [x(t), y(t), z(t), \phi(t), \theta(t), \psi(t)]$$

and

$$\mathbf{v}(t) = [u(t), v(t), w(t), p(t), q(t), r(t)]$$

where t is the time variable, $\boldsymbol{\eta}(t)$ denotes the position and orientation of the vehicle in the world system, and $\mathbf{v}(t)$ is the vector of linear (u is surge velocity, v is sway velocity and w is heave velocity) and angular velocities (p is roll rate, q is pitch rate and r is yaw rate). See Figure 1.

The mathematical model for the equations of motion is based on Gertler and Hagen's [12] six degree of freedom (DOF) submarine equations of motion, which were revised by Feldman [6]. Adapting these general equations to the particular characteristics of a prototype developed by the company Navantia S.A. Shipyard Spain, a very similar coefficient based hydrodynamic model was analyzed in [11, 15]. This latter model will be the starting point for the more general model that we will introduce in this section. For a detailed description of these equations and the value of the hydrodynamic coefficients and the geometric parameters we refer to [11, 14].

A. Blowing and venting model

As shown in Figure 2, the blowing-venting system is composed of ballast tank, pressure bottle, blowing valve and venting valve. When the blowing valve is opened, air flows into the tank increasing the pressure and forcing the water to flow out through the flood port located at the bottom of the tank. When the venting valve is opened, air can flow out from the tank. The model can be divided into four parts:

- Air flow from pressure bottle.
- Air flow through venting valve.
- Water flow through flood port.
- Evolution of pressure in ballast tank.

Variables and symbols introduced in this section are summarized in Table I.

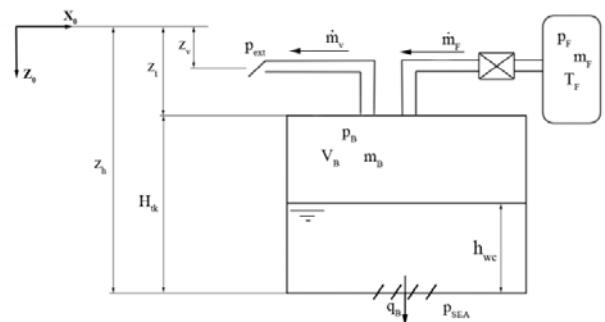


Fig. 2 Blowing and venting processes.

TABLE I. VARIABLES AND SYMBOLS

A	Area in nozzle throat (m^2)
A_h	Outlet hole area (m^2)
A_v	Venting pipe cross-section (m^2)
C_h	Outlet hole coefficient
H_{tk}	Ballast tank height (m)
$h_{wc}(t)$	Height of water column in tank (m)
$m_B(t)$	Mass of air in ballast tank (kg)
$m_F(t)$	Mass of air in pressure bottle (kg)
$\dot{m}_F(t)$	Mass flow rate from pressure bottle (kg/s)
$\dot{m}_v(t)$	Mass flow rate through venting valve (kg/s)
$p_B(t)$	Pressure in ballast tank (Pa)
$p_{ext}(t)$	Pressure outside the venting system (Pa)
$p_F(t)$	Pressure in bottle (Pa)
$p_{SEA}(t)$	Pressure outside the outlet hole (Pa)
$q_b(t)$	Water flow through outlet hole (m^3/s)
T_B	Water temperature (K)
$T_F(t)$	Temperature in pressure bottle (K)
V_{B0}	Initial air volume in ballast tank (m^3)
$V_B(t)$	Volume of air in ballast tank (m^3)

V_{BB}	Ballast tank volume (m ³)
V_F	Pressure bottle volume (m ³)
(x_b, y_b, z_b)	Location of tank geometrical center (m)
z_h	Outlet hole distance from origin (m)
z_t	Tank top distance from origin (m)
z_v	Venting valve distance from origin (m)
γ	Isentropic constant
ρ	Seawater density (kg/m ³)

1) Air flow from pressure bottle.

When the blowing valve is opened, the air in the bottle is blown into the tank through a nozzle. Pressure losses and heat transfer in the tube that connects the bottle and the tank are, for the moment, neglected. However, as we will see later on, pressure losses can be indirectly taken into account. Under the above conditions, we need to study the one dimensional steady flow of an ideal compressible gas. This can be found in any classic text on fluid mechanics (see for example [4]) so that we include next the resulting equation (see also [8] for more details):

$$\dot{m}_F(t) = A \left(\frac{m_F(t)^{\gamma+1}}{m_{F0}^\gamma V_F} \right) \mu(p_B(t), m_F(t)) \quad (1)$$

with

$$\mu(p_B, m_F) = \begin{cases} \sqrt{\gamma \left(\frac{2}{\gamma+1} \right)^{\frac{\gamma+1}{\gamma-1}}}, & p_c \leq \frac{p_F}{p_B} \\ \frac{2\gamma}{\gamma-1} \left(\left(\frac{p_B}{p_{F0} \left(\frac{m_F}{m_{F0}} \right)^\gamma} \right)^{\frac{2}{\gamma}} - \left(\frac{p_B}{p_{F0} \left(\frac{m_F}{m_{F0}} \right)^\gamma} \right)^{\frac{\gamma+1}{\gamma}} \right), & 1 < \frac{p_F}{p_B} < p_c \\ 0, & \frac{p_F}{p_B} \leq 1 \end{cases}$$

Since the initial mass flow rate depends only on the initial conditions in the bottle, it can be considered as a constant with value

$$\dot{m}_F(0) = A \left(\gamma \left(\frac{2}{\gamma+1} \right)^{\frac{\gamma+1}{\gamma-1}} \frac{p_{F0} m_{F0}}{V_F} \right)^{\frac{1}{2}} \quad (2)$$

This initial mass flow rate has been measured for several blowing intensities. Let \dot{m}_{Fmax} be this measured maximum mass flow rate. Then we take

$$A = \dot{m}_{Fmax} \left(\left(\frac{2}{\gamma+1} \right)^{\frac{\gamma+1}{\gamma-1}} \frac{V_F}{\gamma p_{F0} m_{F0}} \right)^{\frac{1}{2}} \quad (3)$$

By doing so, we ensure that the initial mass flow rate calculated coincides with the real measured value. This way, although pressure losses are not considered in the model, they are indirectly taken into account.

2) Air flow through venting valve.

Equations for the air flow from the tank can be obtained analogously to the ones used for the mass flow from the bottle. The variation in the mass of air in the ballast tank is the difference between the mass flow rate from the bottle and the mass flow rate through the venting valve. Thus,

$$\dot{m}_B(t) = -\dot{m}_F(t) - \bar{\mu}(\Pi(t)) \frac{A_v p_B(t)}{\sqrt{R_g T_B(t)}} \quad (4)$$

where $\Pi(t) = \frac{p_{ext}(t)}{p_B(t)}$, $p_{ext}(t) = p_{atm} + \rho g(z + z_v - x_b \sin \theta)$ being the pressure outside the venting valve, and

$$\bar{\mu}(\Pi) = \begin{cases} \bar{\mu}_{max}, & \Pi \leq \Pi_{crit} \\ \frac{-66.97\Pi^2 - 52.70\Pi + 119.70}{\Pi^3 - 171.30\Pi^2 - 75.65\Pi + 294.60}, & \Pi_{crit} < \Pi < 1 \\ 0, & \Pi \geq 1 \end{cases}$$

with $\Pi_{crit} = 0.158$ and $\bar{\mu}_{max} = 0.355$. Since the geometric details of the venting system are not available and therefore pressure losses can not be directly calculated, the above expression for $\bar{\mu}(\Pi)$ has been obtained using a least squares fit of experimental data.

3) Water flow through flood port.

The difference between the tank and outside pressure forces the water to flow in or out from the tank through the flood port located at the bottom. Let us assume, in the first place, that the pressure in ballast tank is greater than the outside pressure. Then, the water flows out from the tank. A detailed analysis of a draining tank filled with an ideal fluid can be found in [4]. From Bernoulli's equation applied at both sides of the port, the volume flow from the ballast tank is given by

$$q_B(t) = C_h A_h \sqrt{\frac{2(p_B(t) + \rho g h_{wc}(t) - p_{SEA}(t))}{\rho(1 + \zeta_h)}}, \quad (5)$$

where A_h is the outlet hole area and C_h is a coefficient that takes into account that, since the outlet hole is actually a grid, the effective area is smaller than A_h . Finally, h_{wc} is the height of the water column in the tank and the estimated coefficient $\zeta_h = 2.5$ accounts for pressure losses in the outlet hole. We refer to [8] for more details. If pressure in ballast tank is lower than the outside pressure, then water flows into the tank. In this case, the expression for the volume flow changes its sign.

4) Evolution of pressure in ballast tank.

When the blowing valve is opened the air is blown into the tank at a very high velocity, rapidly mixing with water. This promotes good heat transfer from the water to the expanding air and thus we may assume that the air will immediately adopt the temperature in the tank. The process can then be considered to be isothermal. As mentioned in [2], experimental results sustain this assumption. From the ideal gas law and the perfect gas equation it follows that the variation in tank pressure is given by

$$\dot{p}_B(t) - \frac{p_B(t)}{m_B(t)} \dot{m}_B(t) = -\frac{p_B^2(t) q_B(t)}{m_B(t) R_g T_B} \quad (6)$$

At the mathematical and numerical levels, the presence of the square root in this equation generates serious difficulties. Indeed, if the term inside the square root vanishes, then the gradient blows-up. To overcome this difficulty we have approximated the square root near the origin by a fourth-order polynomial

$$P(x) = 8.75x^2 - 14x^3 + 6.25x^4$$

that preserves the average volume flow. To sum up, we consider the new function

$$\bar{P}(x) = \begin{cases} -\sqrt{-x} & \text{if } x < -1 \\ -P(-x) & \text{if } -1 \leq x \leq 0 \\ P(x) & \text{if } 0 < x \leq 1 \\ \sqrt{x} & \text{if } x > 1 \end{cases}$$

and replace $q_B(t)$ by

$$\bar{q}_B(t) = C_h A_h \bar{P} \left(\frac{2(p_B(t) + \rho g h_{wc}(t) - p_{SEA}(t))}{\rho(1 + \zeta_h)} \right). \quad (7)$$

5) *Blowing and venting controlled system.*

Once a model for blowing and venting operations has been presented, our next goal is to use such a system as a control mechanism to improve the manoeuvrability of the vehicle. To this end, we introduce a new set of variables: the control variables of the blowing-venting system. Let $s_i, \bar{s}_i \in L^\infty(0, t_f; [0, 1])$ denote, respectively, the grade of aperture of blowing and venting valves of the i -th ballast tank during the time interval $[0, t_f]$. Introducing these control variables in the above equations we obtain the following set of equations for each tank governing the *controlled* evolution of the mass of air in each pressure bottle, the mass of air in the corresponding tank, and its pressure:

$$\dot{m}_{F_i}(t) = s_i A \left(\frac{m_{F_i}(t)^{\gamma+1}}{m_{F_0}^\gamma V_F} \right) \mu_i(p_{B_i}(t), m_{F_i}(t)) \quad (8)$$

$$\dot{m}_{B_i}(t) = -\dot{m}_{F_i}(t) - \bar{\mu}_i(\Pi(t)) \frac{\bar{s}_i A_v p_B(t)}{\sqrt{R_g T_B}} \quad (9)$$

$$\dot{p}_{B_i}(t) - \frac{p_{B_i}(t)}{m_{B_i}(t)} \dot{m}_{B_i}(t) = -\frac{p_{B_i}^2(t) \bar{q}_{B_i}(t)}{m_{B_i}(t) R_g T_B} \quad (10)$$

The above formulation assumes that the flow through the valves varies linearly with their aperture. Of course, once the control system were implemented in a real vehicle this assumption should be adapted to the particular characteristics of the chosen valves. The values of all the required geometrical parameters for the four tanks considered here are summarized in Table II.

TABLE III. BALLAST TANKS CHARACTERISTICS

	MBT 2	MBT 3	MBT 4	MBT 5
A_h	0.191	0.191	0.191	0.191
A_v	0.0177	0.0177	0.0177	0.0177
C_h	0.7	0.7	0.7	0.7
H_{tk}	5	5	5	5
p_{F_0}	$2.5 \cdot 10^7$	$2.5 \cdot 10^7$	$2.5 \cdot 10^7$	$2.5 \cdot 10^7$
T_{F_0}	293	293	293	293
V_{B_0}	0.001	0.001	0.001	0.001
V_{BB}	21.4	21.4	22.9	22.9
V_F	0.8	0.8	0.8	0.8
x_b	-28.6	-28.6	23	23
y_b	1.2	-1.2	1.7	-1.7
z_b	0.595	0.595	0.975	0.975
z_h	-2.895	-2.895	-3.897	-3.897
z_t	2.105	2.105	2.303	2.303
z_v	2.705	2.705	2.705	2.705

B. *Coupling of Blowing-Venting System With a Variable Mass Model for the Equations Of Motion*

As water flows in or out of the tanks there will be mass variations located at several points of the vehicle. It is necessary to account for these mass variations in the equations of motion. In the first place, it is necessary to identify which terms, formerly constant, will become time dependent due to its dependence with mass. In this respect, we need to write mass, weight, moments and products of inertia and location of the center of gravity as a function of the amount of water in the tanks. Secondly, since both the mass and the inertia tensor are now time varying, terms of the form $\frac{dm}{dt}x$ and $\frac{dl}{dt}x$ will appear in the conservation laws for linear and angular momentum together with the terms $m\dot{x}$ and $m\dot{l}$.

Let us assume there are N ballast tanks with geometrical centers located at points (x_{bi}, y_{bi}, z_{bi}) (where the subscript i denotes the i -th ballast tank). Let m_0 be the initial mass of the submarine (with all tanks completely filled with water) and Δm_i the mass loss in the i -th tank. It is 0 when the tank is completely filled with water, and reaches its maximum value when it empties. The volume of water that has left the tank is equal to the volume occupied by air except for the initial air volume in the tank, V_{B_0} , which depends on the initial mass of air in the tank, m_{B_0} , and the initial depth. Thus,

$$\begin{aligned} \Delta m_i(t) &= \rho(V_{B_i}(t) - V_{B_0}) \\ &= \rho \left(\frac{m_{B_i}(t) R_g T_B}{p_{B_i}(t)} - V_{B_0} \right). \end{aligned} \quad (11)$$

Consequently,

$$m(t) = m_0 - \sum_{i=1}^N \Delta m_i(t) \text{ and } W(t) = gm(t) \quad (12)$$

with g the acceleration due to gravity.

Although the vehicle buoyancy B is usually assumed to be constant, it is really a function of the vehicle depth since as depth increases, outside pressure compresses the vehicle. Let B_0 be the buoyancy at zero depth. The buoyancy is assumed to be linearly dependent with respect to the vehicle depth in the form

$$B = B_0 \left(1 - \frac{0.0015}{300} \right) z.$$

To find expressions for the location of the center of gravity and moments and products of inertia we assume that the mass loss in each tank occurs at a point $(x_{bi}, y_{bi}, z_{mli}(t))$ where $z_{mli}(t)$ is the height at which mass loss happens for each tank. It varies from the top of the tank, when it is completely filled, to its geometric center z_{bi} when it is completely empty. This variation is assumed to be linear so that

$$z_{mli}(t) = z_{ti} - \frac{(z_{ti} - z_{bi}) \Delta m_i(t)}{\Delta m_{i,max}}$$

where z_{ti} is the location of the tank top and $\Delta m_{i,max}$ is the maximum value of the mass loss. From this, it is easy to

express the time variation of moments, products of inertia and coordinates of the center of gravity. For instance,

$$\begin{aligned} I_x(t) &= I_{x0} - \sum_{i=1}^N (y_{bi}^2 + z_{mli}(t)^2) \Delta m_i(t), \\ I_{xz}(t) &= I_{xz0} - \sum_{i=1}^N x_{bi} z_{mli}(t) \Delta m_i(t), \\ x_G &= \frac{1}{m_0 - \sum_{i=1}^N \Delta m_i(t)} \left(m_0 x_{G0} - \sum_{i=1}^N x_{bi} \Delta m_i(t) \right), \end{aligned} \quad (13)$$

where the subscript 0 corresponds to parameters with tanks completely filled.

Regarding the terms $\frac{dm}{dt}x$ and $\frac{dl}{dt}x$, they can be considered negligible. Indeed, the time derivatives of vehicle mass and inertia tensor components are

$$\begin{aligned} \frac{dm}{dt} &= \rho R_g T_B \sum_{i=1}^N \left(\frac{m_{Bi}(t) \dot{p}_{Bi}(t)}{p_{Bi}(t)^2} - \frac{\dot{m}_{Bi}(t)}{p_{Bi}(t)} \right), \\ \frac{dI_z(t)}{dt} &= \rho R_g T_B \sum_{i=1}^N (x_{bi}^2 + y_{bi}^2) \left(\frac{m_{Bi}(t) \dot{p}_{Bi}(t)}{p_{Bi}(t)^2} - \frac{\dot{m}_{Bi}(t)}{p_{Bi}(t)} \right). \end{aligned}$$

The maximum rate of change in vehicle mass takes place at the beginning of blowing, when the flow rate from bottle is maximum and the entrance of air in the tank causes an overpressure. Experimental results allow us to estimate this overpressure in about a 15 % at a depth of 100 m. Hence, since the mass flow rate from bottle is maximum, $\dot{m}_B = -\dot{m}_{F,max}$, and taking into account the values in Table 2, we obtain an upper bound for the variation of mass of around $6 \cdot 10^3$ kg/s. Hence, comparing this with the initial mass and the initial moments of inertia (see [14]), even if the derivatives of the state variables are one order of magnitude lower than these, the terms $\frac{dm}{dt}x$ and $\frac{dl}{dt}x$ are two orders of magnitude lower than the terms $m\dot{x}$ and $m\dot{l}$. This sustains the idea of using a quasi-steady variable mass model.

C. Complete model in compact form

Summarizing, the state variables of the system can be expressed in vector form as

$$\mathbf{x}(t) = [[m_{Fi}(t), m_{Bi}(t), p_{Bi}(t)]_{1 \leq i \leq N}, \boldsymbol{\eta}(t)^T, \mathbf{v}(t)^T]^T$$

and the control vector

$$\mathbf{u}(t) = [s_i(t), \bar{s}_i(t)]_{1 \leq i \leq N}^T$$

represents the aperture of blowing and venting valves.

Finally, the state law is composed of equations (8)-(10) for the blowing-venting system, the kinematic and dynamic equations of motion (see [6, 11]), where the time variable parameters as described in Subsection II.B have been taken into account. In compact form we write these equations as

$$\mathbf{A}(\mathbf{x}(t))\dot{\mathbf{x}}(t) = \mathbf{f}(t, \mathbf{x}(t), \mathbf{u}(t)), \quad (14)$$

where $\mathbf{A}(\mathbf{x}(t))$ is a matrix of size $(3N + 12) \times (3N + 12)$ and $\mathbf{f}(t, \mathbf{x}(t), \mathbf{u}(t))$ is a vector of size $(3N + 12)$ for every $t \geq 0$. In Section IV we will analyze in detail the structure of \mathbf{A} and \mathbf{f} . Nevertheless, at this point, it is

convenient to comment on the explicit dependence of \mathbf{f} with respect to the time variable. Since we plan to analyze the potential use of blowing-venting as a control system for manoeuvrability, deflection of bow plane $\delta_b(t)$, deflection of stern plane $\delta_s(t)$, deflection of rudder $\delta_r(t)$, and propeller speed $n(t)$, that typically are the elements used for the manoeuvrability of the submarine, will be fixed to some convenient values during the whole time of manoeuvre. More precisely, we assume that $\delta_b, \delta_s, \delta_r, n \in L^\infty(0, t_f; \mathcal{H})$, where

$$\mathcal{H} = \left[-\frac{5\pi}{36}, \frac{5\pi}{36} \right] \times \left[-\frac{5\pi}{36}, \frac{5\pi}{36} \right] \times \left[-\frac{7\pi}{36}, \frac{7\pi}{36} \right] \times [0, 2.5].$$

Therefore, the explicit dependence of \mathbf{f} on time is linked to these four functions.

III. FORMULATION OF THE CONTROL PROBLEM

Next, we plan to analyze the potential use of blowing-venting operations as a control mechanism in a typical emergency rising manoeuvre where the submarine must reach surface quickly while keeping its stability. Given an initial state $\mathbf{x}(0) = \mathbf{x}^0$ and a desired final target \mathbf{x}^{t_f} , the goal is to calculate the vector of control $\mathbf{u} = \mathbf{u}(t)$, which is able to draw our system from the initial state \mathbf{x}^0 to (or near to) the final one \mathbf{x}^{t_f} in a given time t_f , also minimizing a cost functional. In mathematical terms we have the Bolza-type problem

$$\left\{ \begin{array}{l} \text{Minimize in } \mathbf{u}: \\ J(\mathbf{u}) = \Phi(\mathbf{x}(t_f), \mathbf{x}^{t_f}) + \int_0^{t_f} F(t, \mathbf{x}(t)) dt \\ \text{subject to} \\ \mathbf{A}(\mathbf{x}(t))\dot{\mathbf{x}}(t) = \mathbf{f}(t, \mathbf{x}(t), \mathbf{u}(t)) \\ \mathbf{x}(0) = \mathbf{x}^0, \mathbf{x}(t) \in \Omega \\ 0 \leq s_i(t), \bar{s}_i(t) \leq 1, \quad 1 \leq i \leq N \end{array} \right. \quad (P_{t_f})$$

where Ω stands for the set of constraints for the state variable. Typically

$$\Phi(\mathbf{x}(t_f)) = \sum_{j=1}^{3N+12} \alpha_j (x_j(t_f) - x_j^{t_f})^2 \quad (15)$$

with $\alpha_j \geq 0$ penalty parameters, and

$$F(t, \mathbf{x}(t)) = \sum_{j=1}^{3N+12} \beta_j (x_j(t) - \bar{x}_j(t))^2 \quad (16)$$

with $\beta_j \geq 0$ also weight parameters and $\bar{\mathbf{x}}(t) = [\bar{x}_j(t)]$ a desired trajectory.

The set Ω , which models the constraints on the state variable, has the following structure. For the variables entering in the blowing-venting model, since the outside pressure at a certain depth is the sum of the atmospheric pressure and the weight of the water column above the submarine, even if the pressure in the ballast tank is slightly lower than the outside pressure and the vehicle is close to the surface, we can safely assume that the pressure in the tank will always be greater than the atmospheric pressure, that is $p_{Bi} \geq p_{\bar{B}} = p_{atm}$. Although an upper bound can not be so easily obtained, it is easy to see that the pressure in the

tank will always take finite values, which justifies the assumption $p_{B_i} \leq p_B^+ < \infty$. It is also immediate to see that the upper bound for the mass of air in the tank and bottle is the initial mass of air in the bottle. By hypothesis, there will always be a residual amount of air in the tanks, m_{B_0} . Therefore $m_{B_i} \geq m_B^- = m_{B_0} > 0$. As we stated before, the pressure in the tank will not drop below p_{atm} . Since the air will flow due to the pressure difference between bottle and tank, the pressure in the bottle will have the same lower bound. This way, using the perfect gas equation a lower bound for the air mass in the bottle can be obtained, $m_{F_i} \geq m_F^- > 0$. Summarizing, we are able to assume the constraints

$$\begin{cases} 0 < m_F^- \leq m_{F_i} \leq m_F^+ < +\infty \\ 0 < m_B^- \leq m_{B_i} \leq m_B^+ < +\infty \\ 0 < p_B^- \leq p_{B_i} \leq p_B^+ < +\infty. \end{cases} \quad (17)$$

As for Euler angles, since we are dealing with a manned submarine, typically

$$-\frac{\pi}{4} < \phi < \frac{\pi}{4}, \quad -\frac{\pi}{4} < \theta < \frac{\pi}{4}, \quad 0 < \psi < 2\pi.$$

Due to the bounded nature of the ocean, the position components (x, y, z) are also limited to some bounded rectangle. Finally, the physics of the problem also imposes a constraint on the rest of components (ie. linear (u, v, w) and angular (p, q, r) velocities).

To sum up, we can assume that Ω is a bounded rectangle.

IV. MATHEMATICAL ANALYSIS

We start our analysis by proving that for any initial state $\mathbf{x}^0 \in \Omega$ and any admissible control $\mathbf{u}(t)$ there exists a unique solution of (14) starting from \mathbf{x}^0 , and also satisfying $\mathbf{x}(t) \in \Omega$, defined in some interval $0 \leq t \leq t_f$ where $t_f = t_f(\mathbf{x}^0)$ only depends on the initial condition. However, since the state law is expressed in implicit form, we can not apply standard results. To overcome this difficulty we will show that the matrix-valued map \mathbf{A} is smooth and takes nonsingular values, that is, the state law can be rewritten in explicit form as

$$\dot{\mathbf{x}}(t) = \mathbf{A}(\mathbf{x}(t))^{-1} \mathbf{f}(t, \mathbf{x}(t), \mathbf{u}(t)). \quad (18)$$

A. \mathbf{A} is Nonsingular-Valued

It is clear that for any $\mathbf{x} \in \Omega$ and any admissible control $\mathbf{u}(t)$, the matrix $\mathbf{A}(\mathbf{x})$ has the form

$$\mathbf{A}(\mathbf{x}) = \begin{bmatrix} \mathbf{BV}(\mathbf{x}) & \mathbf{0}_{3N \times 6} & \mathbf{0}_{3N \times 6} \\ \mathbf{0}_{6 \times 3N} & I_6 & \mathbf{0}_{6 \times 6} \\ \mathbf{0}_{6 \times 3N} & \mathbf{0}_{6 \times 6} & \mathbf{M}(\mathbf{x}) \end{bmatrix} \quad (19)$$

where $\mathbf{BV}(\mathbf{x})$ is the submatrix associated to the blowing-venting equations and $\mathbf{M}(\mathbf{x})$ is the so called (variable) inertia matrix. Furthermore, $\mathbf{BV}(\mathbf{x})$ is a $3N \times 3N$ matrix structured in 3×3 diagonal blocks

$$\mathbf{BV}(\mathbf{x}) = \begin{bmatrix} \mathbf{BV}_1(\mathbf{x}) & \cdots & \mathbf{0}_{3 \times 3} \\ \vdots & \ddots & \vdots \\ \mathbf{0}_{3 \times 3} & \cdots & \mathbf{BV}_N(\mathbf{x}) \end{bmatrix} \quad (20)$$

where, for $1 \leq i \leq N$,

$$\mathbf{BV}_i(\mathbf{x}) = \begin{bmatrix} 1 & 0 & 0 \\ 1 & 1 & 0 \\ 0 & -1 & \frac{m_{B_i}}{p_{B_i}} \end{bmatrix} \quad (21)$$

with $\det \mathbf{BV}_i(\mathbf{x}) = \frac{m_{B_i}}{p_{B_i}} \geq \frac{m_B^-}{p_B^+} > 0$ by (17). Thus $\mathbf{BV}_i(\mathbf{x})$ is nonsingular with

$$\mathbf{BV}_i(\mathbf{x})^{-1} = \begin{bmatrix} 1 & 0 & 0 \\ -1 & 1 & 0 \\ \frac{-p_{B_i}}{m_{B_i}} & \frac{p_{B_i}}{m_{B_i}} & \frac{p_{B_i}}{m_{B_i}} \end{bmatrix} \quad (22)$$

and, therefore, the full matrix $\mathbf{BV}(\mathbf{x})$ is also nonsingular for every admissible state $\mathbf{x} \in \Omega$ with

$$\mathbf{BV}(\mathbf{x})^{-1} = \begin{bmatrix} \mathbf{BV}_1(\mathbf{x})^{-1} & \cdots & \mathbf{0}_{3 \times 3} \\ \vdots & \ddots & \vdots \\ \mathbf{0}_{3 \times 3} & \cdots & \mathbf{BV}_N(\mathbf{x})^{-1} \end{bmatrix}. \quad (23)$$

It just remains to prove that the inertia matrix \mathbf{M} is invertible. From the dynamic equations of motion and (12)-(13) we have that $\mathbf{M}(\mathbf{x})$ has the form

$$\mathbf{M}(\mathbf{x}) = \mathbf{M}_v(\mathbf{x}) + \mathbf{M}_c \quad (24)$$

where

$$\mathbf{M}_v(\mathbf{x}) = \begin{bmatrix} m(\mathbf{x})I_3 & -\mathbf{S}(\mathbf{x}) \\ \mathbf{S}(\mathbf{x}) & \mathbf{I}(\mathbf{x}) \end{bmatrix} \quad (25)$$

is the variable part of the matrix, with

$$\mathbf{S}(\mathbf{x}) = \begin{bmatrix} 0 & -m(\mathbf{x})z_G(\mathbf{x}) & m(\mathbf{x})y_G(\mathbf{x}) \\ m(\mathbf{x})z_G(\mathbf{x}) & 0 & -m(\mathbf{x})x_G(\mathbf{x}) \\ -m(\mathbf{x})y_G(\mathbf{x}) & m(\mathbf{x})x_G(\mathbf{x}) & 0 \end{bmatrix}$$

and

$$\mathbf{I}(\mathbf{x}) = \begin{bmatrix} I_x(\mathbf{x}) & -I_{xy}(\mathbf{x}) & -I_{xz}(\mathbf{x}) \\ -I_{xy}(\mathbf{x}) & I_y(\mathbf{x}) & -I_{yz}(\mathbf{x}) \\ -I_{xz}(\mathbf{x}) & -I_{yz}(\mathbf{x}) & I_z(\mathbf{x}) \end{bmatrix}$$

the inertia tensor, and \mathbf{M}_c is the so-called added inertia matrix (see [11]).

It is usual in the literature on dynamics of submerged vehicles (see [8, Property 2.4], for instance) to assume that \mathbf{M}_c is a symmetric and positive definite matrix (and therefore invertible). However, experimental values of the non-dimensional hydrodynamic coefficients reported by Navantia showed that this is not a realistic assumption in all cases. In particular the inertia matrix used in our numerical experiments, based in the experimental data provided by Navantia, is not symmetric, but it is invertible.

Let \mathbf{M}_0 be the rigid-body inertia matrix of the submarine with all the ballast tanks completely filled with water, i.e.,

$$\mathbf{M}_0 = \begin{bmatrix} m_0 I_3 & m_0 \begin{bmatrix} 0 & z_{G0} & -y_{G0} \\ -z_{G0} & 0 & x_{G0} \\ y_{G0} & -x_{G0} & 0 \end{bmatrix} \\ m_0 \begin{bmatrix} 0 & -z_{G0} & y_{G0} \\ z_{G0} & 0 & -x_{G0} \\ -y_{G0} & x_{G0} & 0 \end{bmatrix} & \mathbf{I}_0 \end{bmatrix}$$

This matrix is symmetric and usually is assumed to be

positive definite ([8, Property 2.2]). Therefore whenever matrices \mathbf{M}_c and \mathbf{M}_0 are assumed to be symmetric and positive definite, the inertia matrix $\mathbf{M}_0 + \mathbf{M}_c$ is invertible, since it is also symmetric and positive definite. Otherwise the invertibility of $\mathbf{M}_0 + \mathbf{M}_c$ must be checked for any particular model.

Finally, nonsingularity of $\mathbf{M}(\mathbf{x})$ follows from the next classical Lemma.

LEMMA III.1 Let $\mathbf{D} \in \mathcal{M}^{m \times m}$ be an invertible matrix and let $\Delta \in \mathcal{M}^{m \times m}$ be a square matrix such that

$$\|\mathbf{D}^{-1}\Delta\| = \sup\{|\mathbf{D}^{-1}\Delta\mathbf{y}| : |\mathbf{y}| = 1\} < 1$$

where $|\cdot|$ denotes the Euclidian norm in \mathbb{R}^m . Then $\mathbf{D} + \Delta$ is invertible with

$$(\mathbf{D} + \Delta)^{-1} = \sum_{n=0}^{\infty} (-1)^n (\mathbf{D}^{-1}\Delta)^n \mathbf{D}^{-1}$$

Computing the operator norm of a matrix is not in general an easy task, but next well-known Lemma provides a very useful estimate.

LEMMA III.2 Let $\mathbf{D} = [d_{ij}] \in \mathcal{M}^{m \times m}$ be a square matrix. Then

$$\|\mathbf{D}\| \leq \sqrt{\sum_{i,j} d_{ij}^2}. \tag{26}$$

The right-hand side in (26) is called the Frobenius norm of \mathbf{D} , $\|\mathbf{D}\|_F$.

Let $\mathbf{x} \in \Omega$ be an admissible state. Since $\mathbf{M}(\mathbf{x}) = (\mathbf{M}_0 + \mathbf{M}_c) + (\mathbf{M}_v(\mathbf{x}) - \mathbf{M}_0)$ with $\mathbf{M}_0 + \mathbf{M}_c$ invertible, by Lemma 1, it suffices to show that

$$\|(\mathbf{M}_0 + \mathbf{M}_c)^{-1} + (\mathbf{M}_v(\mathbf{x}) - \mathbf{M}_0)\| < 1 \tag{27}$$

to have the nonsingularity of $\mathbf{M}(\mathbf{x})$. Furthermore, Lemma 1 also ensures that

$$\mathbf{M}(\mathbf{x})^{-1} = \sum_{n=0}^{\infty} (-1)^n ((\mathbf{M}_0 + \mathbf{M}_c)^{-1} + (\mathbf{M}_v(\mathbf{x}) - \mathbf{M}_0))^n \cdot (\mathbf{M}_0 + \mathbf{M}_c)^{-1}. \tag{28}$$

Summarizing, $\mathbf{M}(\mathbf{x})$ is invertible, for any state $\mathbf{x} \in \Omega$, whenever $\mathbf{M}_0 + \mathbf{M}_c$ is invertible and the variation of mass due to the blowing-venting manoeuvres is small enough. More precisely, if

$$\Delta m^+ < \frac{\lambda_{min}}{\sqrt{3 + 4N \sum_{i=1}^N |\mathbf{c}_i|^2 + \frac{9}{2} \sum_{i=1}^N |\mathbf{c}_i|^4}} \tag{29}$$

holds, where $\Delta m^+ = \sum_{i=1}^N \Delta m_{i,max} = \rho \sum_{i=1}^N (V_{BBi} - V_{B0})$ is the maximum variation of mass, $\lambda_{min} > 0$ is the smallest singular value of the inertia matrix $\mathbf{M}_0 + \mathbf{M}_c$ and \mathbf{c}_i is the geometrical center of the i -th ballast tank, then \mathbf{M} is nonsingular-valued.

THEOREM III.4. If the matrix $\mathbf{M}_0 + \mathbf{M}_c$ is invertible and the inequality (28) is satisfied, then the matrix-valued map $\mathbf{A} : \Omega \rightarrow \mathcal{M}^{(12+3N) \times (12+3N)}$ takes nonsingular values, that is, $\mathbf{A}(\mathbf{x})$ is invertible for any $\mathbf{x} \in \Omega$ with

$$\mathbf{A}(\mathbf{x})^{-1} = \begin{bmatrix} \mathbf{B}\mathbf{V}(\mathbf{x})^{-1} & \mathbf{0}_{3N \times 6} & \mathbf{0}_{3N \times 6} \\ \mathbf{0}_{6 \times 3N} & I_6 & \mathbf{0}_{6 \times 6} \\ \mathbf{0}_{6 \times 3N} & \mathbf{0}_{6 \times 6} & \mathbf{M}(\mathbf{x})^{-1} \end{bmatrix}.$$

Moreover, the map $\mathbf{x} \rightarrow \mathbf{A}(\mathbf{x})^{-1}$ is continuously differentiable.

Proof. To show that $\mathbf{A}(\mathbf{x})$ is invertible for any $\mathbf{x} \in \Omega$, it suffices to show that (27) is satisfied uniformly with respect to the state variable. We have

$$\begin{aligned} \|(\mathbf{M}_0 + \mathbf{M}_c)^{-1} + (\mathbf{M}_v(\mathbf{x}) - \mathbf{M}_0)\| &\leq \|(\mathbf{M}_0 + \mathbf{M}_c)^{-1}\| \|\mathbf{M}_v(\mathbf{x}) - \mathbf{M}_0\| \\ &= \frac{1}{\lambda} \|\mathbf{M}_v(\mathbf{x}) - \mathbf{M}_0\| \end{aligned}$$

by properties of the matrix norm (see [16, Appendix A], for instance). Let us now obtain estimates for the supremum of the Frobenius norm of the variable matrix. Firstly, from (11)

$$\left| \sum_{i=1}^N \Delta m_i(\mathbf{x}) \right| \leq \sum_{i=1}^N \Delta m_{i,max} = \rho \sum_{i=1}^N (V_{BBi} - V_{B0}). \tag{30}$$

Let us now estimate the variation of the coordinates of the center of gravity

$$\left| \sum_{i=1}^N x_{bi} \Delta m_i(\mathbf{x}) \right| \leq (\Delta m^+) \sum_{i=1}^N |x_{bi}|, \tag{31}$$

$$\left| \sum_{i=1}^N y_{bi} \Delta m_i(\mathbf{x}) \right| \leq (\Delta m^+) \sum_{i=1}^N |y_{bi}|, \tag{32}$$

$$\left| \sum_{i=1}^N z_{mi} \Delta m_i(\mathbf{x}) \right| \leq (\Delta m^+) \sum_{i=1}^N |z_{bi}| \tag{33}$$

with (x_{bi}, y_{bi}, z_{bi}) the coordinates of the geometrical center of the i -th tank. Finally, from (13) and (30)

$$\begin{aligned} |I_x(\mathbf{x}) - I_{x0}| &= \left| \sum_{i=1}^N (y_{bi}^2 + z_{mi}^2) \Delta m_i(\mathbf{x}) \right| \\ &\leq (\Delta m^+) \sum_{i=1}^N (y_{bi}^2 + z_{bi}^2) \end{aligned} \tag{34}$$

Similar estimates can be obtained for the rest of moments and products of inertia.

Hence, from Lemma 2 and estimates (30)-(34), it follows that for any $\mathbf{x} \in \Omega$,

$$\begin{aligned} \|\mathbf{M}_v(\mathbf{x}) - \mathbf{M}_0\| &\leq (\Delta m^+) \sqrt{3 + 4N \left(\sum_{i=1}^N x_{bi}^2 + y_{bi}^2 + z_{bi}^2 \right) + \frac{9}{2} \left(\sum_{i=1}^N x_{bi}^2 + y_{bi}^2 + z_{bi}^2 \right)^2} \end{aligned}$$

where we have also used the convexity inequality

$$(\sum_{i=1}^N a_i)^2 \leq N(\sum_{i=1}^N a_i^2) \text{ and also that } ab \leq (a^2 + b^2)/2.$$

Combining this inequality with (29), we have the desired inequality (27). Finally, from (23) and (28) it follows that $\mathbf{x} \rightarrow \mathbf{A}(\mathbf{x})^{-1}$ is continuously differentiable and the proof is complete. \square

Remark 1. For the particular data of the prototype considered in our numerical experiments, $\mathbf{M}_0 + \mathbf{M}_c$ is invertible. Moreover, $\lambda_{min} = 1.54 \cdot 10^{12}$ and hence

$$(\Delta m^+) \sqrt{\frac{3 + 4N(\sum_{i=1}^N x_{bi}^2 + y_{bi}^2 + z_{bi}^2) + \frac{9}{2}(\sum_{i=1}^N x_{bi}^2 + y_{bi}^2 + z_{bi}^2)^2}{\lambda_{min}}} = 1.73 \cdot 10^{-4}.$$

B. The state law is well-posed

Set $K = [0,1]^{2N}$. An admissible control of the problem will be an essentially bounded map taking values in K , that is, $L^\infty(0, +\infty; K)$ is the space of admissible controls. Given $\mathbf{u} \in L^\infty(0, +\infty; K)$, our aim in this section is to show that the system (18) has a solution for any initial state \mathbf{x}^0 . We begin by recalling the classical theory on this subject. For the details we refer the reader to [16, Appendix C].

By a (Carathéodory) solution we mean an absolutely continuous function $t \rightarrow \mathbf{x}(t) \in \Omega$, defined on some interval $I = [0, t_f]$, which satisfies the integral equation

$$\mathbf{x}(t) = \mathbf{x}^0 + \int_0^t \mathbf{g}(s, \mathbf{x}(s)) ds, \quad \text{for every } t \in [0, t_f]$$

where, for simplicity, we write $\mathbf{g}: I \times \Omega \rightarrow \mathbb{R}^{3N+12}$, $\mathbf{g}(t, \mathbf{x}) = \mathbf{A}(\mathbf{x}(t))^{-1} \mathbf{f}(t, \mathbf{x}(t), \mathbf{u}(t))$.

We recall that the solution $\mathbf{x}(t)$ defined on $[0, t_f]$ is said to be maximal if t_f is the largest time for which $\mathbf{x}(t)$ is defined. As it is well-known, if \mathbf{g} satisfies conditions (H1)-(H4) below, then we can ensure the existence and uniqueness of a maximal solution of (18) for any initial state:

- (H1) For each $\mathbf{x} \in \Omega$, the function $\mathbf{g}(\cdot, \mathbf{x}): I \rightarrow \mathbb{R}^N$ is measurable.
- (H2) For each $t \in I$, the function $\mathbf{g}(t, \cdot): I \rightarrow \mathbb{R}^N$ is continuous.
- (H3) \mathbf{g} is locally Lipschitz with respect to \mathbf{x} that is, for each $\mathbf{x}^0 \in \Omega$ there exist a real number $\varepsilon > 0$ and a locally integrable function $\alpha: I \rightarrow \mathbb{R}^+$ such that the ball $B_\varepsilon(\mathbf{x}^0)$ of radius ε centered at \mathbf{x}^0 is contained in Ω and

$$|\mathbf{g}(t, \mathbf{x}) - \mathbf{g}(t, \mathbf{y})| \leq \alpha(t) |\mathbf{x} - \mathbf{y}| \quad \text{for every } t \in I \text{ and } \mathbf{x}, \mathbf{y} \in B_\varepsilon(\mathbf{x}^0) \quad (35)$$

- (H4) \mathbf{g} is locally integrable with respect to t , that is, for each $\mathbf{x}^0 \in \Omega$ there exist a locally integrable function $\beta: I \rightarrow \mathbb{R}^+$ such that

$$|\mathbf{g}(t, \mathbf{x}^0)| \leq \beta(t) \text{ a.e. } t \in I. \quad (36)$$

Our main result in this section follows:

THEOREM IV.5. For each $\mathbf{x}^0 \in \Omega$ and each $\mathbf{u} \in L^\infty(0, +\infty; K)$ we can ensure the existence and uniqueness of a solution of (18) which is defined on a maximal time interval $[0, t_f]$, where $t_f = t_f(\mathbf{x}^0)$ only depends on the initial state \mathbf{x}^0 and is uniform with respect to the control $\mathbf{u} \in L^\infty(0, +\infty; K)$.

Proof. To begin with, we notice that thanks to Theorem 1 we may restrict the analysis that follows to the right-hand side of the state law (14). Let us prove that conditions (H1)-(H4) above hold. Since the time variable t only appears in

the control functions $(s_i(t), \bar{s}_i(t))$, $1 \leq i \leq N$, and, by hypothesis, these functions belong to $L^\infty(\mathbb{R}^+; [0,1])$ it is clear that for each $\mathbf{x} \in \Omega$ the function $t \rightarrow \mathbf{f}(t, \mathbf{x})$ is measurable.

As regards the continuity of the function $\mathbf{f}(t, \cdot)$, only the equations modelling the air flow from pressure bottles need of a detailed analysis to check that the pass from supersonic flow to subsonic one is continuous. A direct computation shows that this is so whenever $m_{Fi} \geq m_{\bar{F}} > 0$ and $p_{Bi} \geq p_{\bar{B}} > 0$.

As for condition (H4), from the form in which controls appear in the state law it follows that for each $\mathbf{x}^0 \in \Omega$ the components $f_i(t, \mathbf{x}^0)$, $1 \leq i \leq 3N + 12$, of $\mathbf{f}(t, \mathbf{x}^0)$ are uniformly bounded with respect to t , that is, (36) holds for a constant function $\beta(t) = \beta$ and what is more important, this constant is uniform with respect to $\mathbf{u} \in L^\infty(\mathbb{R}^+; K)$.

Next we analyze the local Lipschitz condition of $\mathbf{f}(t, \mathbf{x})$. Consider firstly the equations f_i , $i = 1 + 3j$, $0 \leq j \leq N - 1$, which model air flow from bottles. Taking into account the set of constraints (17), a direct computation shows that $f_i(t, \cdot) \in W^{1,\infty}(\Omega)$ and therefore they are Lipschitz. As before it is important to notice that the estimates on the partial derivatives of $f_i(t, \cdot)$ are uniform with respect to t , that is, there exists $L > 0$ such that

$$\left| \frac{\partial f_i}{\partial x_j}(t, \mathbf{x}) \right| \leq L \quad (37)$$

for every $\mathbf{x} \in \Omega$ and uniformly w.r.t. $t \geq 0$.

Similarly, functions f_i , $i = 2 + 3j$, $0 \leq j \leq N - 1$, which appear in the equations modelling air flow through venting valve are continuous and satisfy an estimate as in (37). Thus, they are Lipschitz. As before, the Lipschitz constant is uniform with respect to the control variable.

Consider now functions f_{3+3j} , $0 \leq j \leq N - 1$, which appear in the equations for evolution of pressure in ballast tanks. In this case, when pressure in a ballast tank equals outside pressure, the derivatives of velocities in the corresponding flood port blows-up because of the presence of the square root. To avoid this singularity we have approximated the square root as shown in Subsection II.A.4. As a conclusion, once again we obtain that these maps are Lipschitz.

The components f_i , $3N + 1 \leq i \leq 3N + 6$, only include the transformation matrix between body and world reference frames. Taking into account the constraints on Euler angles, it is clear that $f_i \in C^\infty(\Omega)$, $3N + 1 \leq i \leq 3N + 6$, and therefore they are Lipschitz. Notice that the time variable does not appear in these functions.

As for the remaining f_i , $3N + 7 \leq i \leq 3N + 12$, these components include: (a) polynomial terms and terms in the form of absolute values; all of them are Lipschitz, (b) terms like $x_j \sqrt{x_j^2 + x_k^2}$ and $|x_j| \sqrt{x_j^2 + x_k^2}$ for some $18 \leq j \leq 24$. Since these functions are continuous and the discontinuities of its derivatives are of a finite jump, they are also Lipschitz.

(c) Since our model is mass variable, it is necessary to look carefully at the terms including mass m , weight W , center of gravity (x_G, y_G, z_G) and moments and product of inertia $I_x, I_y, I_z, I_{xy} \dots$ because now they depend on some components of the state variable. Taking into account the constraints (17) it is clear that these components are also Lipschitz. Finally, the product of Lipschitz functions is also Lipschitz. As before, these components f_i do not include control variable $\mathbf{u}(t)$ and therefore the corresponding Lipschitz constants are independent of $\mathbf{u}(t)$.

From this analysis it is deduced that for each $\mathbf{x}^0 \in \Omega$ and $\mathbf{u} \in L^\infty(\mathbb{R}^+; K)$ there exists a maximal time $t_f = t_f(\mathbf{x}^0, \mathbf{u})$ and a unique maximal solution defined in $[0, t_f(\mathbf{x}^0, \mathbf{u})]$. Looking at the proof of this existence result (see [16, Th. 36, pp. 347-351]) we realize that t_f depends on \mathbf{u} through the functions $\alpha(t) = \alpha(\mathbf{u}(t))$ and $\beta(t) = \beta(\mathbf{u}(t))$ which appear in (35) and (36). However, as shown before these functions α and β can be chosen uniformly w.r.t. $\mathbf{u} \in L^\infty(\mathbb{R}^+; K)$. As a conclusion, $t_f = t_f(\mathbf{x}^0)$ only depends on the initial condition. This completes the proof. \square

C. Existence of Solution for the Optimal Control Problem

Fix $\mathbf{x}^0 \in \Omega$ and let $t_f = t_f(\mathbf{x}^0)$ be the maximal time, as given by Theorem IV.5, for which system (18) is well-posed. The goal of this section is to prove the following existence result:

THEOREM IV.6. *Let $\mathbf{x}^0 \in \Omega$ and let $0 < t_f = t_f(\mathbf{x}^0) < +\infty$ be as above. Then, there exists, at least, one solution to (P_{t_f}) .*

Proof. The proof follows as a consequence of the classical Filippov existence theorem for Bolza-type optimal control problems (see [3, Th. 9.3.i, p. 314]). Indeed, let us see that the sufficient conditions for the existence of a solution hold. Due to the constraints on the state variable, the set $A = [0, t_f] \times \Omega$ is compact. Similarly, since the set $K = [0, 1]^{2N}$ for control constraints is compact, the set $A \times K$ is also compact. In addition, the function $\Phi: A \times A \rightarrow \mathbb{R}$ defined by (15) is continuous. Continuity also holds for the functions F and \mathbf{g} both defined on $A \times K$.

Notice also that, by Theorem 2, the set of admissible solutions for (P_{t_f}) is not empty. Finally, we must check that for each $(t, \mathbf{x}) \in A$ the orientator field

$$Q(t, \mathbf{x}) = \{ (z^0; \mathbf{z}) \in \mathbb{R}^{1+3N+12}: z^0 \geq F(t, \mathbf{x}), \mathbf{z} = \mathbf{g}(t, \mathbf{x}, \mathbf{u}), \text{ with } \mathbf{u} \in K \}$$

is convex. This convexity easily follows from the facts that the control variable \mathbf{u} appears in a linear form in the state law and the set K is convex. \square

V. NUMERICAL ANALYSIS

A. Algorithm of minimization

There are several optimization methods which can be applied to solve (P_{t_f}) . Due to the complexity of the state law and the large number of variables involved in the

problem, it is quite reasonable to use a gradient descent method with projection. Briefly, the scheme of this method consists of the following main steps:

1. Initialization of the control input \mathbf{u}^0 .
2. For $k \geq 0$, iteration until convergence (e.g. $|J(\mathbf{u}^{k+1}) - J(\mathbf{u}^k)| \leq \varepsilon |J(\mathbf{u}^0)|$, with $\varepsilon > 0$ a suitable tolerance) as follows:

- 2.1. We consider the vector

$$\mathbf{v}^{k+1} = \mathbf{u}^k - \lambda \nabla J(\mathbf{u}^k)$$

where $\lambda > 0$ is a fixed step parameter, and ∇J is the gradient of the cost function.

- 2.2. Since \mathbf{v}^{k+1} may not be admissible, we compute its orthogonal projection onto the admissibility set K , the unit rectangle in \mathbb{R}^8 , that is, $\mathbf{u}^{k+1} = P_K(\mathbf{v}^{k+1})$ where

$$u_j^{k+1} = \min(\max(0, v_j^{k+1}), 1).$$

The crucial step is the computation of the gradient $\nabla J(\mathbf{u}^k)$. This can be obtained by using the adjoint method which is described next:

1. Given the control $\mathbf{u}^k, k \geq 0$, solve the state equation

$$\begin{cases} \mathbf{A}(\mathbf{x}(t)) \dot{\mathbf{x}}(t) = \mathbf{f}(t, \mathbf{x}(t), \mathbf{u}^k(t)) \\ \mathbf{x}(0) = \mathbf{x}^k(0) \end{cases}$$

to obtain the state $\mathbf{x}^{k+1}(t)$.

2. With the pair $(\mathbf{u}^k(t), \mathbf{x}^{k+1}(t))$, solve the linear backward equation for the adjoint state $\mathbf{p}(t)$

$$\begin{cases} \mathbf{A}(\mathbf{x}^{k+1}(t))^T \dot{\mathbf{p}}(t) = -\nabla_x F(t, \mathbf{x}^{k+1}(t), \mathbf{u}^k(t)) \\ \quad - [\nabla_x \mathbf{f}(t, \mathbf{x}^{k+1}(t), \mathbf{u}^k(t))]^T \mathbf{p}(t) \\ \mathbf{A}(\mathbf{x}^{k+1}(t_f))^T \mathbf{p}(t_f) = \nabla_x \Phi(\mathbf{x}^{k+1}(t_f), \mathbf{x}^{t_f}) \end{cases}$$

where ∇_x is the gradient with respect to the state variable \mathbf{x} . Thus, we obtain $\mathbf{p}^{k+1}(t)$.

3. Finally,

$$\begin{aligned} & \nabla J(\mathbf{u}^k) \\ &= \nabla_{\mathbf{u}} F(t, \mathbf{x}^{k+1}(t), \mathbf{u}^k(t)) \\ &+ [\nabla_{\mathbf{u}} \mathbf{f}(t, \mathbf{x}^{k+1}(t), \mathbf{u}^k(t))]^T \mathbf{p}^{k+1}(t) \end{aligned}$$

where now $\nabla_{\mathbf{u}}$ is the gradient with respect to \mathbf{u} .

We refer the reader to [5] for more details on this method.

B. A Numerical Experiment

In order to test the proposed models, this section shows the results of the numerical simulation of an emergency rising manoeuvre. These results are used to analyze both the mathematical properties and the possible real-world applications of the proposed scheme. At each iteration of the gradient algorithm, the numerical resolutions of the state and adjoint state equations have been carried out by using the ODE45 Matlab function, which is a one-step solver based on an explicit Runge-Kutta method.

The typical protocol for an emergency rising is to use the control planes to pitch the nose of the submarine up, increase the speed, and blow the ballast tanks to reduce the weight of the submarine and drive it to the surface with buoyancy. As analyzed in [1, 18], small to medium size submarines exhibit a roll instability during these kind of manoeuvres. Roll angles of up to 25degrees have been reported. It is also known that if the submarine emerges with a high roll angle, it may experiment large roll oscillations on the surface. Of course, this is an undesirable situation, particularly if the operators are attending to the original problem that required the emergency rise.

For these reasons, it might be interesting to check if this situation can be prevented by using blowing/venting control instead of a manual blowing. To this end, an emergency rising manoeuvre has been simulated for three different scenarios:

Scenario 1: A standard manoeuvre. Initial depth is 100 m, initial speed is 2 m/s. Starting from $t = 0$, the protocol described above is used to drive the vehicle to the surface: propeller revolutions are increased to the maximum value, 2.5 rps, to increase the forward speed, and stern and bow planes are set to -20 and 20 degrees respectively; a value selected to rapidly pitch the vehicle up while ensuring that pitch angle is kept within acceptable values. At the same time, ballast tanks 2-5 are simultaneously blown with half the maximum intensity (this corresponds to $s_i = 0.5$ in our model). Vent valves remain closed ($\bar{s}_i = 0.5$) throughout all the simulation. Simulation ends when submarine reaches a depth of 10 m (an arbitrarily low value for which we can assume that the vehicle has reached the surface). To sum up:

$$\begin{aligned} \delta_r(t) &= 0 \\ \delta_s(t) &= -20 \\ \delta_b(t) &= 20 \\ n(t) &= 2.5 \\ s_i &= 0.5, \quad i = 1 \dots 4 \\ \bar{s}_i &= 0, \quad i = 1 \dots 4 \end{aligned} \quad \forall t$$

We note that, although we refer to this scenario as *standard manoeuvre*, the constant value for the deflection of control planes is of course a simplification of what would be done in real operation.

Scenario 2: Same manoeuvre, with the control algorithm acting from $t = 0$ to $t = 30$ s using exclusively the blowing valves. The controls from Scenario1 are used as initialization and the optimization process looks to achieve three main objectives:

- Submarine must rise in a similar time as it does in the standard manoeuvre.
- Rising pitch angle must be around 20 degrees and never above 25 degrees.
- Roll angle must be as close as possible to zero throughout all the simulation.

Scenario 3: Same as Scenario 2 but incorporating the use of venting valves in conjunction with blowing valves.

For both Scenario 2 and Scenario 3, the following set of parameters is used:

$$\begin{cases} \mathbf{x}(0) = ([m_{F0i}, m_{B0i}, p_{B0i}]_{1 \leq i \leq 4}, 0, 0, 100, 0, 0, 0, 2, 0, 0, 0, 0) \\ t_f = 30 \text{ s} \\ \bar{\phi}(t) = \bar{x}_{16}(t) = 0 \quad \forall t \in [0, 30] \\ z^{t_f} = x_{15}^{t_f} = 75, \quad \theta^{t_f} = x_{17}^{t_f} = 10. \\ \alpha_{15} = \alpha_{17} = 1, \quad \alpha_j = 0, j \neq 15, 17. \\ \beta_{16} = 5, \quad \beta_j = 0, j \neq 16. \\ \lambda = 0.001 \quad \varepsilon = 10^{-5} \end{cases}$$

where the initial mass of air in the bottles is $m_{F0i} = 237.8376$ kg, the initial mass of air in the tanks is $m_{B0i} = 0.0126$ kg and the initial pressure in the tanks is $p_{B0i} = 1.0846 \cdot 10^6$ Pa. After $t = 30$ s, simulation continues with fixed controls (values equal to those used in Scenario 1) until the submarine reaches a depth of 10 m.

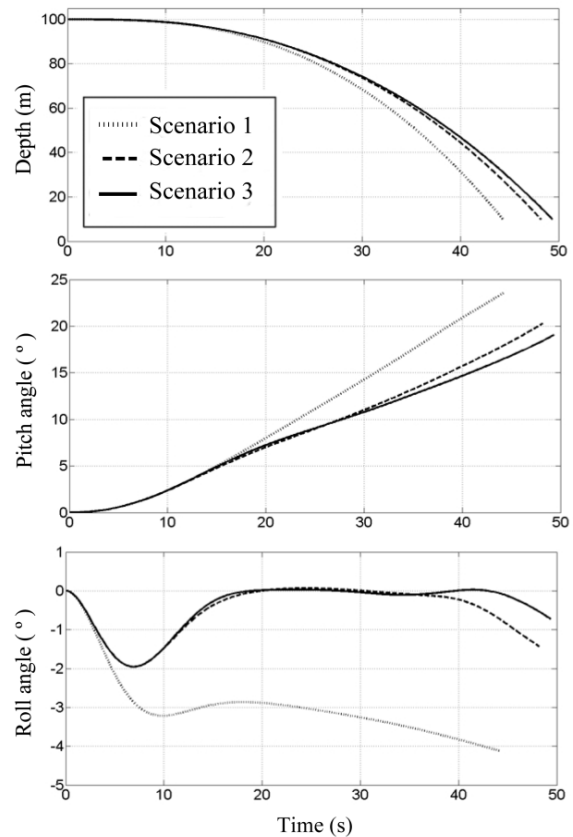


Fig.1 Depth (top), pitch and roll angle (bottom) for Scenario 1 (dotted line), Scenario 2 (dashed line) and Scenario 3 (solid line).

Results are shown in figures 3-6. Figure 3 shows vehicle depth, pitch angle and roll angle for all three scenarios. The rest of state variables have not been included since they are not directly relevant for this particular manoeuvre. Comparison between dotted (standard manoeuvre) and dashed lines (Scenario 2) shows that the three objectives have been achieved for Scenario2: the rising time is only a few seconds greater than in the standard manoeuvre, the final pitch angle is close to 20 degrees and the roll angle has been significantly reduced with respect to the standard manoeuvre. Indeed, Scenario1 exhibits roll angles in the range of 3-4 degrees during most of the simulation time while in Scenario2, after an initial peak of 2 degrees, the roll angle is kept within extremely low values. Results of Scenario 3 (solid line) show that performance can be further

improved by incorporating the aperture of venting valves into the control variable. From the engineering point of view, the convenience of the use of venting during an emergency rise can be arguable and is indeed not a usual practice. However, it is used in Scenario 3 to demonstrate the algorithm capabilities. Table 3 summarizes the value of cost function for standard and optimal controls.

TABLE III. VALUE OF COST FUNCTION FOR STANDARD AND OPTIMAL CONTROLS

Scenario	1	2	3
Cost	1211.447	129.0241	125.1811

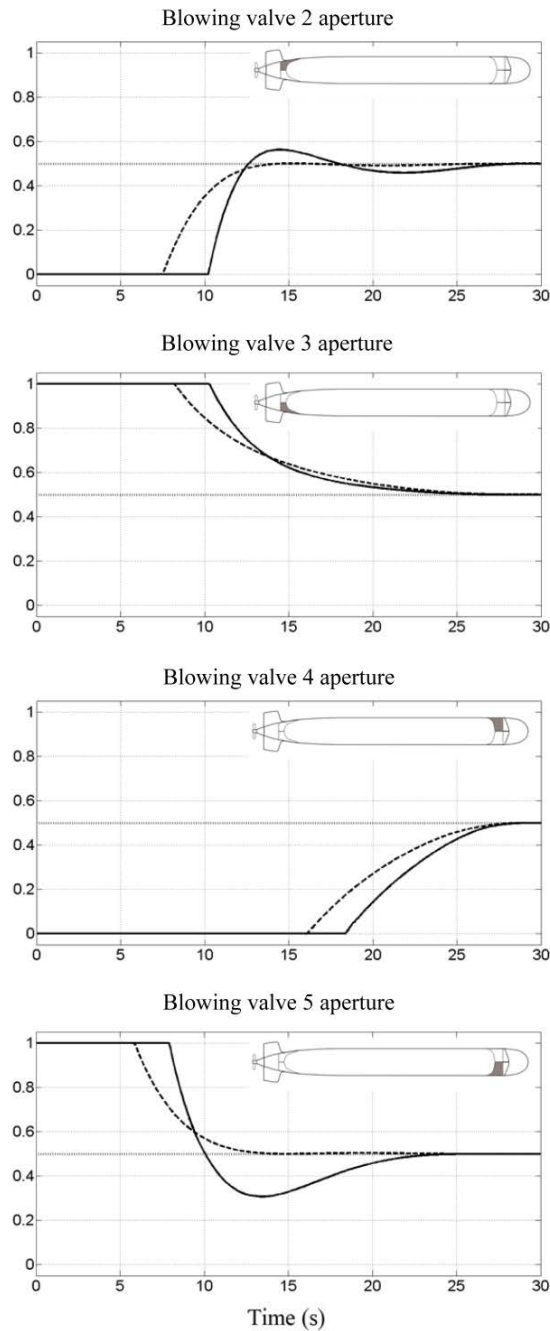


Fig. 4 Blowing valve aperture for standard (dotted lines) and optimal controls (dashed lines for Scenario 2 and solid lines for Scenario 3).

The control variables are shown in figures 4 (blowing valves) and 5 (venting valves). As we can see, the rolling

moment is compensated by blowing more ballast from the starboard tanks. It may surprise that tanks 2 and 4 are being vented while there is no blowing air yet and that, for some time intervals, the same tank is simultaneously blown and vented, but it is worth noting that opening the venting valve changes the pressure against the air is blown. This seems to allow for smoother transitions. Indeed, although taking simultaneously two opposite actions may seem inefficient, the use of venting valves seems to improve the results obtained by using only the blowing valves. Anyway, the results obtained in this test represent an optimum without any engineering considerations; it gives a reference of the best achievable result. This way a better understanding of these manoeuvres and its associated difficulties may be gained. At a practical point of view and having in mind a real implementation in a submarine, engineering considerations may later be easily taken into account by including them in the cost function.

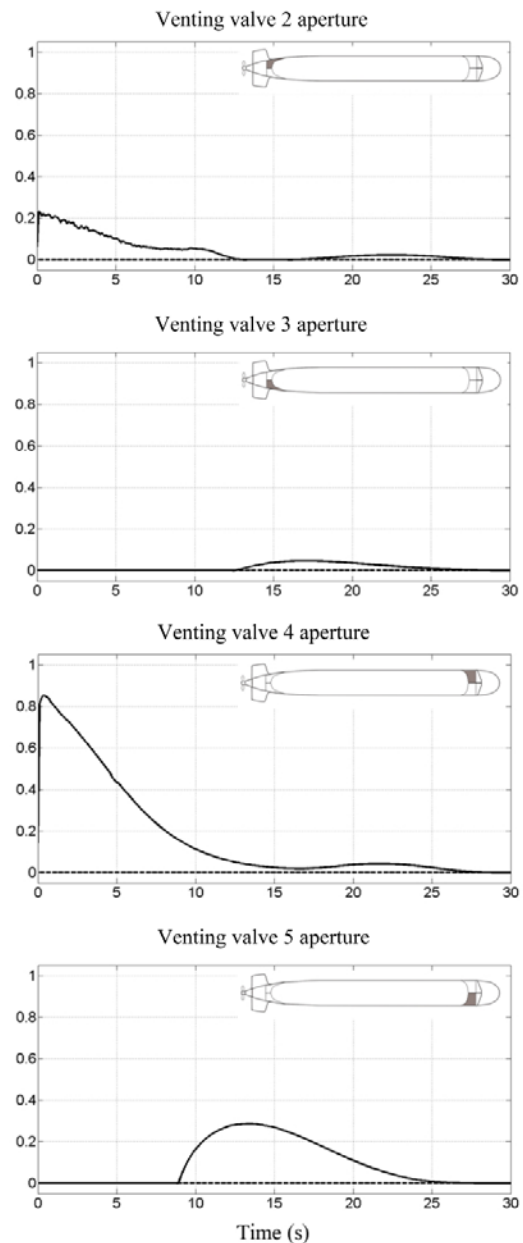


Fig. 5 Venting valve aperture for standard (dotted lines) and optimal controls (dashed lines for Scenario 2 and solid lines for Scenario 3).

The value of the cost function for Scenario 3 at each iteration is plotted in Figure 6. As we see, the algorithm shows exponential convergence. As is usual in this type of algorithm, results depend on the initialization. Different initializations were tested obtaining different optimal controls. This seems to show the existence of several local and/or global minima.

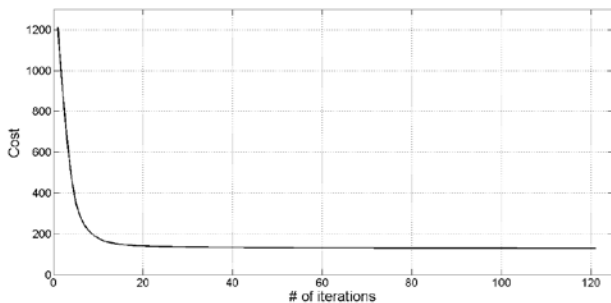


Fig. 6 Cost function at each iteration.

VI. CONCLUSIONS

A quasi-steady mathematical model has been proposed for the coupling of blowing and venting operations with the usual Feldman equations of motion for a conventional manned submarine. This model extends the one proposed in [1,18] where only blowing was considered. A simplified version of our model was announced by the authors in [8]. However, up to the best knowledge of the authors, a mathematical model for coupled blowing and venting operations acting as a control mechanism as presented in this paper has not been studied so far. A detailed mathematical analysis of the model includes the proof of existence of a solution for the resulting system of 24 nonlinear ordinary differential equations. As an illustration of the potential use of the model, we have considered the problem of roll control in an emergency rising manoeuvre. To this end, a suitable optimal control problem has been formulated, the existence of a solution has been obtained and its numerical resolution has been carried out by using a descent algorithm. Numerical simulation results have shown that, indeed, blowing and venting processes in manned submarines are promising devices for manoeuvrability that may be used in a number of real-world applications in naval engineering such as launch and recovery of AUVs.

ACKNOWLEDGMENT

Work supported by projects 2989/10MAE from Navantia S. A. and 08720/PI/08 from Fundación Séneca, Agencia de Ciencia y Tecnología de la Región de Murcia (Programa de Generación de Conocimiento Científico de Excelencia, IIPCTRM 2007-10). The last author was supported by project MTM2007-62945 from Ministerio de Educación y Ciencia (Spain).

REFERENCES

M. C. Bettle, A. G. Gerber, and G. D. Watt, "Unsteady analysis of the six DOF motion of a buoyantly rising submarine", *Computers and Fluids*, 38:1833-1849, 2009.

- L. Bystrom, "Submarine recovery in case of flooding", *Naval Forces*, XXV, 2004.
- L. Cesari, *Optimization theory and applications. Applications of Mathematics*, 17. Springer-Verlag, New York Heidelberg Berlin, 1983.
- C. T. Crowe, D. F. Elger, and J. A. Roberson, *Engineering Fluid Mechanics*, 8th edition. John Wiley & sons, 2004.
- J. C. Culioli, *Introduction a l'optimisation*. Editions Ellipses, Paris, 1994.
- J. Feldman, "Revised standard submarine equations of motion". Report DTNSRDC/SPD-0393-09. David W. Taylor Naval Ship Research and Development Center, WashingtonDC, 1979.
- R. Font, J. García, and D. Ovalle, Modeling and simulating ballast tank blowing and venting operations in manned submarines. In *8th IFAC Conference on Control Applications in Marine Systems*, Rostock-Warnemünde, Germany, 2010.
- R. Font, J. García and J. A. Murillo, A mathematical model for the analysis and control of ballast tank blowing and venting operations in manned submarines. In *XXII CEDYA*, Palma de Mallorca, Spain, 2011.
- T. I. Fossen, *Guidance and control of ocean vehicles*. John Wiley & sons, WashingtonDC, 1994.
- R. Fraga and L. Sheng, "An effective state-space feedback autopilot for ship motion control", *JCET Vol. 2 N° 2*, pp.62-69, April 2012.
- J. García, D. Ovalle, and F. Periago, "Analysis and numerical simulation of a nonlinear mathematical model for testing the manoeuvrability capabilities of a submarine", *NonLinear Analysis: Real World Applications*, Vol. 12, pp. 1654-1669, 2011.
- M. Gertler and G. R. Hagen, "Standard equations of motion for submarine simulation". NSRDC Report 2510, 1967.
- I. Lasiacka and Y. Lu, "Stabilization of a nonlinear fluid structure interaction via feedback controls and geometry of the domain", *JCET Vol. 2 N° 4*, pp. 143-153, October 2012.
- D. Ovalle, Nonlinear optimal control strategies for maneuverability analysis of manned submarines, thesis, Universidad Politécnica de Cartagena, Spain, 2011.
- F. Periago and J. Tiago, "A local existence result for an optimal control problem modelling the manoeuvring of an underwater vehicle", *Nonlinear Analysis: Real World Applications*, Vol. 11, pp. 2573-2583, 2010.
- E. Sontag, *Mathematical control theory*, Texts in Applied Mathematics, 6. Springer-Verlag, New York, USA, 1990.
- G.D. Watt, A quasi-steady evaluation of submarine rising stability: the stability limit. In *RTO-AVT symposium on advanced flow management*. Loen, Norway, 2001.
- G.D. Watt, "Modelling and simulating unsteady six degrees-of-freedom submarine rising maneuvers". DRDC Atlantic TR 2007-08, 2007.



Roberto Font received his Ph. D. degree at the Universidad Politécnica de Cartagena, Spain, in 2013. This work is part of his Ph. D. in collaboration with the company Navantia S. A.

His research interest focuses on mathematical modeling and simulation, nonlinear and optimal control, optimal design and engineering applications, particularly in the field of

underwater vehicles.



Javier García-Peláez is Naval Architect & Marine Engineer for the Universidad Politécnica de Madrid, Spain.

He holds in Navantia the current position of Head of Submarine Preliminary Design Department. In particular, he has been responsible for Hydrodynamics and Signatures Management of the Submarine

Projects for this company during the last decade.



José Alberto Murillo received his Ph. D. degree in applied mathematics at the University of Valencia, Spain, in 1998. He was a postdoctoral fellow at the Ecole Polytechnique in Paris, France, supported by the European Community's Improving Human Potential Programme (2003/04). He is currently Assistant Professor at the Department of Applied

Mathematics and Statistics of the Technical University of Cartagena, Spain.

He has published research papers in referred journals. His research interests range over viability theory, control, nonsmooth and set-valued analysis and shape dynamics, as well as real-world applications, mainly in engineering.

Dr. Murillo is a member of SEMA (Spanish Society for Applied Mathematics) and SIAM.



Francisco Peria received his Ph. D. degree in applied mathematics in 1999 at the University of Valencia, Spain. He was a postdoctoral fellow at University of New South Wales, Sydney (Australia) in 2000. Currently he is an Assistant Professor at the Department of Applied Mathematics and Statistics of the Universidad Politécnica de Cartagena, Spain.

He has published over 20 research papers in referred journals. His main research interest includes Optimal Control, Optimal Design and Controllability, both at the theoretical level and for its application to real-world engineering problems. Between 2008 and 2012 he was responsible for the research projects 2113/07MAE and 2989/10MAE, in collaboration with the company NAVANTIA S.A for the improvement of the design and manoeuvrability of manned submarines. He is a member of SEMA (Spanish Society for Applied Mathematics).